Catalysis Science & Technology

ROYAL SOCIETY OF CHEMISTRY

COMMUNICATION

View Article Online
View Journal | View Issue

Check for updates

Cite this: *Catal. Sci. Technol.*, 2024, **14**, 1756

Received 27th December 2023,
Accepted 22nd February 2024

DOI: 10.1039/d3cy01785k

rsc.li/catalysis

Open Access Article. Published on 27 February 2024. Downloaded on 4/4/2026 11:54:14 PM.
This article is licensed under a Creative Commons Attribution 3.0 Unported Licence.

Boosting photocatalytic hydrogen production of CdS/$BiVO_4$ nanoplates by transferring in-plane plasmon resonant energy of gold nanoparticles†

Ming-Han Liu ‡*[ab] and Yukina Takahashi *[abc]

A free-standing plate-type plasmon-enhanced Z-scheme photocatalytic system has been established *via* CdS deposition on Au-decorated $BiVO_4$ nanoplates (CdS/Au on $BiVO_4$). Through the enhancement from in-plane plasmon resonant energy transfer of gold, the hydrogen evolution rate of CdS/Au on $BiVO_4$ was enhanced about 7.7 times higher than that of the gold-free photocatalyst.

Levels of carbon dioxide emissions from the combustion of fossil fuels have steadily increased over time year by year. The development of sustainable energy sources such as hydrogen energy has become a highly attractive topic in the literature due to environmental concerns.[1] Hydrogen is a promising energy carrier due to its high energy density and zero carbon emissions in combustion.[2] Hydrogen can be produced from multiple resources such as natural gas reforming, sugar fermentation and water splitting. Solar energy-driven water splitting is currently economically viable and environmentally benign compared with other energy sources. Since Honda and Fujishima discovered the decomposition of water on TiO_2 electrodes in 1972,[3] semiconducting photocatalysts thus have drawn extensive and increasing attention due to their capabilities to convert solar energy to chemical energy (*i.e.*, forming hydrogen *via* photocatalytic reduction of water). With the exception of TiO_2, the literature has reported numerous photocatalysts for water splitting.[4] As is well known, rapid recombination of photo-generated charge carriers occurring in a single phase photocatalyst leads to a poor quantum efficiency and a low photocatalytic activity. Thus, the improvement of electron–hole separation efficiency of photocatalysts has become an emerging and attractive topic in photocatalysis. There are several strategies to improve the photo-generated charge separation efficiency of photocatalysts, such as impurity doping,[5] construction of heterojunctions,[6–8] and conjugation of plasmonic metals (such as Au, Ag, and Cu).[9,10] Z-Scheme photocatalysts with a heterojunction in between can effectively reduce the recombination of photo-generated charge carriers *via* the formation of an interfacial electric field. Conjugated plasmonic metals on metal oxide surfaces usually give rise to the effects of direct electron transfer (denoted as DET) and plasmon resonant energy transfer (denoted as PRET). The former participates in the plasmonic enhancement effect *via* the injection of hot electrons. The latter is beneficial to charge separation by plasmonic energy transfer. There are numerous studies reporting the enhanced hydrogen production from plasmonic metal-conjugated semiconducting photocatalysts that possess negative conduction band edges enabling reduction of protons, thus producing hydrogen.[9] Among these cases, particulate hybrid photocatalysts exhibited plasmon-enhanced photocatalytic activity boosted by DET and/or PRET. To develop highly efficient photocatalysts for hydrogen evolution, generating plenty of H_2-evolution centers around a plasmonic metal on semiconducting oxide nanoplates is the most feasible strategy.

To the best of our knowledge, very limited attention has been paid to the study of plasmonic enhancement in hydrogen evolution over free-standing Z-scheme nanoplate-type photocatalysts, especially when using a plasmonic metal solely for its enhancing role rather than serving as a shuttle mediator.[11] We choose bismuth vanadate nanoplates ($BiVO_4$ NPs) as a platform to construct a Z-scheme photocatalyst through cadmium sulfide deposition (denoted as CdS/$BiVO_4$). For demonstrating the plasmonic effect, gold nanoparticles were deposited on $BiVO_4$ NPs by photoirradiation prior to the deposition of CdS (denoted as CdS/Au on $BiVO_4$, Scheme 1). For comparison, a thin silica coated gold decorated Z-scheme

[a] *International Institute for Carbon-Neutral Energy Research (WPI-I2CNER), Kyushu University, 744 Moto-oka, Nishi-ku, Fukuoka, 819-0395, Japan. E-mail: yukina@mail.cstm.kyushu-u.ac.jp*
[b] *Mitsui Chemicals, Inc. – Carbon Neutral Research Center (MCI-CNRC), Kyushu University, 744 Moto-oka, Nishi-ku, Fukuoka, 819-0395, Japan*
[c] *Center for Future Chemistry, Kyushu University, 744 Moto-oka, Nishi-ku, Fukuoka 819-0395, Japan*

† Electronic supplementary information (ESI) available. See DOI: https://doi.org/10.1039/d3cy01785k

‡ Present address: Department of Applied Chemistry, National Chiayi University, Chiayi City, 600355, Taiwan. E-mail: mhliu@mail.ncyu.edu.tw

This journal is © The Royal Society of Chemistry 2024

Open Access Article. Published on 27 February 2024. Downloaded on 4/4/2026 11:54:14 PM.
This article is licensed under a Creative Commons Attribution 3.0 Unported Licence.

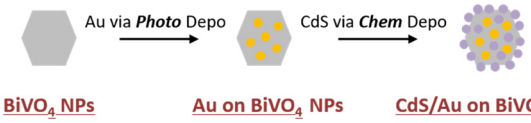

Scheme 1 Schematic demonstrating the synthesis of gold-decorated $BiVO_4$ nanoplate supported CdS photocatalysts through deposition methods, including, photodeposition for gold nanoparticles and chemical deposition for CdS nanoparticles.

photocatalyst (denoted as CdS/SiO_2-capped Au on $BiVO_4$) was prepared in order to exclude the enhancing contribution from the DET mechanism. These Z-scheme photocatalysts were evaluated in hydrogen evolution in the presence of sacrificial agents. The hydrogen evolution rate of CdS/Au on $BiVO_4$ was approximately 7.7 times higher than that of the gold-free photocatalyst, *i.e.*, $CdS/BiVO_4$. Through the analyses of time-resolved photoluminescence spectroscopy, the results indicated that gold decoration effectively improved the separation efficiency of charge carriers, resulting in prolonged carrier lifetimes. Compared with CdS/SiO_2-capped Au on the $BiVO_4$ photocatalyst, it is believed that the dominant enhancing factor in hydrogen evolution is attributed to the PRET mechanism instead of DET.

$BiVO_4$ is a typical semiconductor with a narrow bandgap of *ca.* 2.5 eV and a suitable valence band edge at 2.4 eV *vs.* NHE, providing adequate potential for holes to oxidize water.[12] The $BiVO_4$ nanoplates were prepared according to the literature report[13] with slight modification (see ESI† for the details). The $BiVO_4$ nanoplates exhibit a thickness of *ca.* 40 nm (Fig. 1a) and size ranging from *ca.* 700 nm to 1–2 μm (Fig. 1b). The {010} crystal facets of $BiVO_4$ NPs possess a lower conduction band energy level as compared with other facets, thus accumulating photo-generated electrons for the reduction of $AuCl_4^-$ ions. Fig. 1c shows that the majority of gold nanoparticles have a sphere-like shape and the size is about 12.0 ± 2.8 nm. The deposition of CdS nanoparticles was carried out *via* the assistance of electrostatic interactions between Cd ions and the negatively charged $BiVO_4$ surface. The particle size of CdS is about 11.7 ± 2.3 nm (Fig. 1d). The gold-decorated $CdS/BiVO_4$ photocatalyst was thus constructed through sequential deposition of gold and CdS nanoparticles (Fig. 1e and f). The scanning transmission electron microscope (denoted as STEM) image (Fig. 1e) clearly shows that some CdS nanoparticles are independently located on the surface. Some CdS nanoparticles surrounded the gold due to the thiol group of the precursor, thiourea. STEM with energy-dispersive X-ray spectroscopy (*i.e.*, STEM-EDS) analysis showed that the CdS nanoparticles were deposited only next to the gold rather than on the top surface of the gold (data not shown). After sequential deposition, the {010} facets of $BiVO_4$ NPs existed as usual with only slight unevenness. However, due to the quite uniform deposition of Au and CdS, the surface unevenness is thus not a significant influencing factor in photocatalysis. Furthermore, to exclude the influence from DET, a thin silica layer was introduced to cap the naked gold surface prior to CdS deposition, resulting in the formation of CdS/SiO_2-capped Au on $BiVO_4$ (Fig. S1†). X-ray diffraction (XRD) patterns (Fig. 2a) confirm the deposition and crystal phases of CdS (ICDD no. 00-041-1049) and gold (ICDD no. 00-004-0784). The loading percentage by weight for CdS and Au was estimated as *ca.* 22% and 10%, respectively (Fig. S2†) by using an SEM equipped with an energy dispersive X-ray spectrometer. Through the characterization by diffuse reflectance spectroscopy (Fig. 2b), the absorption spectrum of $CdS/BiVO_4$ is nearly the same as that of pristine $BiVO_4$. Moreover, gold decoration gives rise to an obvious absorption band from 500 to 900 nm due to the distorted spherical shapes of gold. The spectrum without clear peaks is due to the fact that AuNPs with various sizes, shapes, and refractive indices of the surrounding medium, as evidenced by the TEM images (Fig. 1), have arisen. The photocatalytic activity in hydrogen evolution over the as-prepared samples was evaluated (Fig. 3a). In this system, SO_3^{2-} and S^{2-} are oxidized on $BiVO_4$ and water is reduced on CdS to produce hydrogen. The photocatalyst, CdS/Au on $BiVO_4$, shows that the evolution rate of hydrogen, *i.e.*, 2366 μmol g^{-1} h^{-1}, is about 7.7 times higher than that of CdS/$BiVO_4$ (305 μmol g^{-1} h^{-1}). Furthermore, CdS/Au on the $BiVO_4$ photocatalyst was evaluated at different irradiation wavelengths

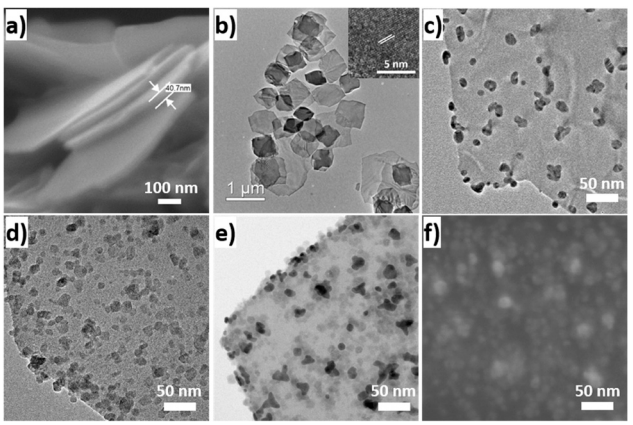

Fig. 1 Scanning electron microscope (SEM) (a) and transmission electron microscope (TEM) (b) images of $BiVO_4$ nanoplates (NPs). TEM images of Au-deposited (c) and CdS-deposited (d) $BiVO_4$ NPs. Scanning-TEM (STEM) (e) and SEM (f) images of Au-deposited $BiVO_4$ NPs, followed by CdS deposition (the inset in (b) shows the lattice fringes of the $BiVO_4$ (200) planes).

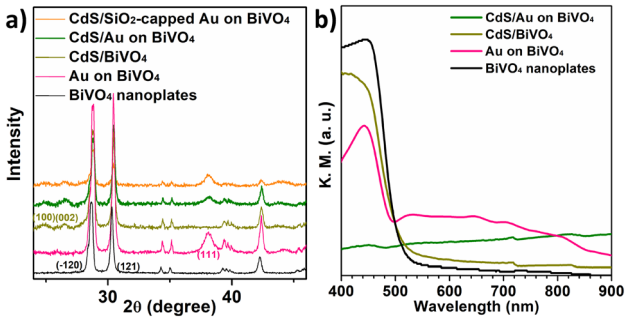

Fig. 2 XRD patterns (a) and diffuse reflectance absorption spectra (b) of the as-prepared photocatalysts (black, brown and pink labels in (a) indicate the crystal facets of $BiVO_4$, CdS, and Au, respectively).

Open Access Article. Published on 27 February 2024. Downloaded on 4/4/2026 11:54:14 PM.
This article is licensed under a Creative Commons Attribution 3.0 Unported Licence.

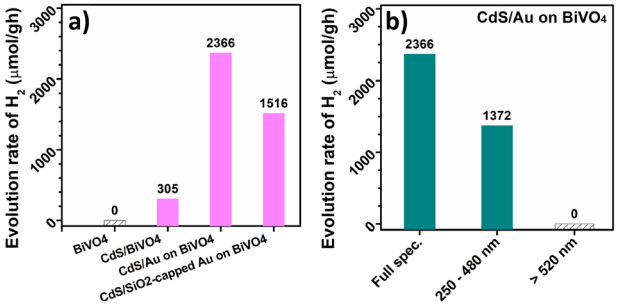

Fig. 3 Photocatalytic hydrogen evolution of $BiVO_4$-based photocatalysts under the full spectrum of the Xe lamp (a) and CdS/Au on $BiVO_4$ at different irradiation wavelengths (b) (the evolution rates of hydrogen were calculated after 6 h of photocatalytic reactions).

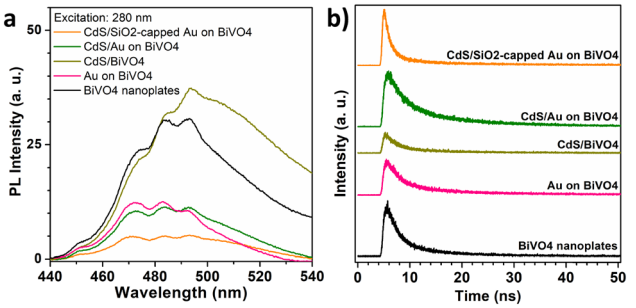

Fig. 4 Steady-state photoluminescence (a) and time-resolved photoluminescence (*i.e.*, TRPL) (b) spectra of the as-prepared samples under 280 nm excitation light (TRPL was monitored at 483 nm).

(Fig. 3b). The evolution rate of hydrogen just remained 58% in the case of unfiltered irradiation, when using irradiation wavelengths ranging from 250 to 480 nm (away from the surface plasmon resonance band of gold nanoparticles) as excitation. The 42% decrease in activity can be ascribed to the removal of any possible influence from the surface plasmon resonance effect (due to its absorption at 500–900 nm). There is no activity under irradiation at a wavelength longer than 520 nm. That is because the irradiation wavelength was completely outside the adsorption window of CdS and $BiVO_4$. Therefore, the photocatalyst was inactive under irradiation at a wavelength longer than 520 nm. Moreover, it was difficult to obtain hydrogen from the $CdS/BiVO_4$ photocatalyst only through the excitation of gold using irradiation light longer than 520 nm. The effective PRET enhancement in the hydrogen evolution of CdS/Au on the $BiVO_4$ photocatalyst only occurred in the presence of efficient dipole–dipole interactions (*i.e.*, spectral overlap) between Au and $CdS/BiVO_4$.[14] According to the literature,[14] the transfer of hot electrons from SPR resonant gold to $BiVO_4$ is not dominant in the system of Au on $BiVO_4$. However, the electron transfer from SPR resonant gold to CdS may occur to produce hydrogen, but the trace amount of hydrogen will be under the detection level based on our experimental conditions. Since $BiVO_4$ exhibits slow charge transportation and high recombination of photo-generated electrons and holes,[15] it is believed that the efficiency of charge carrier separation could be improved obviously through the introduction of gold as a solid redox mediator in Z-scheme photocatalysts.[16] However, in comparison with the evolution rate of CdS/SiO_2-capped Au on $BiVO_4$ (Fig. 3a), it is believed that the plasmonic effect of gold, not the solid redox mediator, is the main factor responsible for improving the hydrogen evolution rate of CdS/Au on the $BiVO_4$ photocatalyst. The DET and PRET plasmonic enhancements are usually entangled together. Therefore, in order to elaborate the enhancement mechanism from gold over the $CdS/BiVO_4$ Z-scheme photocatalyst, we measured the steady-state and time-resolved photoluminescence[17] to investigate the separation efficiency of photo-generated charge carriers over our photocatalysts (Fig. 4a and b). In Fig. 4a, pristine $BiVO_4$ exhibits strong photoluminescence (denoted as PL) peaks at 473, 483, and 494 nm. When gold nanoparticles were deposited on $BiVO_4$, the PL intensities were decreased significantly (pink, olive, and orange lines in Fig. 4a). That is because the lifetimes of photo-generated charge carriers were prolonged. For CdS deposition, the PL intensity of $CdS/BiVO_4$ shows a slight increase accompanied by a slight shape change ranging from 500 to 530 nm due to extra luminescence from CdS. This indicates that $CdS/BiVO_4$ possesses a shortened carrier lifetime. The prolonged carrier lifetime of CdS/Au on $BiVO_4$ is potentially beneficial for photocatalysis, in agreement with its photocatalytic activity. Time-resolved photoluminescence spectroscopy was utilized to analyse the photo-generated charge carriers in-depth (Fig. 4b). Two time constants are extracted from the fitting: fast decay component, τ_1, originating from the electron trapping in the near CB edge of $BiVO_4$ and slow component, τ_2, originating from electron–hole recombination (Table 1). Due to the PL overlap of $BiVO_4$ with CdS in our system, the analysed results of the carrier lifetime are interpreted carefully. All samples exhibit prolonged τ_1 and τ_2 in comparison with that of pristine $BiVO_4$ nanoplates. The longer carrier lifetimes of τ_1 and τ_2 for Au on the $BiVO_4$ sample exhibit that gold decoration can effectively suppress the recombination of electron–hole carriers and prolong the trapping time of electrons in the CB edge of $BiVO_4$. The construction of Z-scheme $CdS/BiVO_4$ also prolongs the carrier lifetime as Au-decorated $BiVO_4$ NPs. The thin silica coating on the gold further improves the separation efficiency of photo-generated charge carriers. According to the analysed data (Table 1), it is clear that the reduction of carrier recombination indicates that PRET mainly dominates the photocatalysis instead of DET in our photocatalysts because if DET is dominant, the recombination rate would increase due to the injection of hot electrons (Fig. 5).

Table 1 Lifetimes of the as-prepared samples obtained *via* fitting of decay PL curves in Fig. 4b using a bi-exponential function

Sample	τ_1 (ns)	τ_2 (ns)
CdS/SiO_2-capped Au on $BiVO_4$	3.0	15.9
CdS/Au on $BiVO_4$	3.5	12.6
$CdS/BiVO_4$	4.5	21.3
Au on $BiVO_4$	3.4	16.3
$BiVO_4$ nanoplates	2.8	10.0

This journal is © The Royal Society of Chemistry 2024

Open Access Article. Published on 27 February 2024. Downloaded on 4/4/2026 11:54:14 PM.
This article is licensed under a Creative Commons Attribution 3.0 Unported Licence.

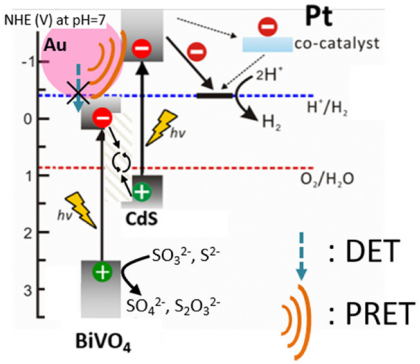

Fig. 5 Schematic illustration of plasmon-enhanced photocatalytic hydrogen evolution over CdS/Au on the $BiVO_4$ photocatalyst (DET: direct electron transfer; PRET: plasmon resonant energy transfer).

This knowledge of the mechanism obtained in this study has made it possible to design an optimal system.

Conclusions

We have successfully utilized free-standing Au-decorated $BiVO_4$ nanoplates as substrates to construct plasmon-enhanced Z-scheme photocatalysts by depositing CdS nanoparticles (CdS/Au on $BiVO_4$). The deposition of CdS nanoparticles occurred on the surface of $BiVO_4$ due to the electrostatic interaction between cadmium ions and the $BiVO_4$ surface. The photocatalytic hydrogen evolution of CdS/Au on the $BiVO_4$ photocatalyst has been effectively increased by about 7.7 times as compared with the gold-free CdS/$BiVO_4$ photocatalyst. The time-resolved photoluminescence spectroscopy analysis indicated that gold decoration improved the separation efficiency of carriers, resulting in the enhancement of hydrogen evolution. This enhancement is attributed to the in-plane plasmon resonant energy transfer not the direct electron transfer. We believe that this in-plane plasmon-enhanced Z-scheme photocatalytic system could provide ideas for designing various highly efficient two-dimensional plasmonic photocatalysts in the near future.

We gratefully acknowledge the funding for this work from Mitsui Chemicals, Inc. M.-H. Liu thanks Dr. Masaki Kudo (The Ultramicroscopy Research Center, Kyushu University) and Mr. Koki Nishimura (Center for Molecular Systems (CMS), Kyushu University) for the assistance in STEM-EDS (M. K.) and TRPL (K. N.) analyses.

Conflicts of interest

There are no conflicts to declare.

References

1 S. E. Hosseini and M. A. Wahid, Hydrogen production from renewable and sustainable energy resources: Promising green energy carrier for clean development, *Renewable Sustainable Energy Rev.*, 2016, **57**, 850–866.
2 J. Graetz, New approaches to hydrogen storage, *Chem. Soc. Rev.*, 2009, **38**, 73–82.
3 A. Fujishima and K. Honda, Electrochemical Photolysis of Water at a Semiconductor Electrode, *Nature*, 1972, **238**, 37–38.
4 Q. Wang and K. Domen, Particulate Photocatalysts for Light-Driven Water Splitting: Mechanisms, Challenges, and Design Strategies, *Chem. Rev.*, 2020, **120**, 919–985.
5 Z. Zhu, W. Shen, D. Li, J. Ye, X. Song, X. Tang, J. Zhao and P. Huo, Oxygen-Doped Red Carbon Nitride: Enhanced Charge Separation and Light Absorption for Robust CO_2 Photoreduction, *Inorg. Chem.*, 2023, **62**, 15432–15439.
6 H. Tada, T. Mitsui, T. Kiyonaga, T. Akita and K. Tanaka, All-solid-state Z-scheme in CdS–Au–TiO_2 three-component nanojunction system, *Nat. Mater.*, 2006, **5**, 782–786.
7 P. Zhou, J. Yu and M. Jaroniec, All-Solid-State Z-Scheme Photocatalytic Systems, *Adv. Mater.*, 2014, **26**, 4920–4935.
8 Z. Zhu, X. Xing, Q. Qi, W. Shen, H. Wu, D. Li, B. Li, J. Liang, X. Tang, J. Zhao, H. Li and P. Huo, Fabrication of graphene modified CeO_2/g-C_3N_4 heterostructures for photocatalytic degradation of organic pollutants, *Chin. J. Struct. Chem.*, 2023, 100194.
9 S. Ezendam, M. Herran, L. Nan, C. Gruber, Y. Kang, F. Gröbmeyer, R. Lin, J. Gargiulo, A. Sousa-Castillo and E. Cortés, Hybrid Plasmonic Nanomaterials for Hydrogen Generation and Carbon Dioxide Reduction, *ACS Energy Lett.*, 2022, **7**, 778–815.
10 T. Kawawaki, T. Nakagawa, M. Sakamoto and T. Teranishi, Carrier-Selective Blocking Layer Synergistically Improves the Plasmonic Enhancement Effect, *J. Am. Chem. Soc.*, 2019, **141**, 8402–8406.
11 J. Long, H. Chang, Q. Gu, J. Xu, L. Fan, S. Wang, Y. Zhou, W. Wei, L. Huang, X. Wang, P. Liu and W. Huang, Gold-plasmon enhanced solar-to-hydrogen conversion on the {001} facets of anatase TiO2 nanosheets, *Energy Environ. Sci.*, 2014, **7**, 973–977.
12 Y. Park, K. J. McDonald and K.-S. Choi, Progress in bismuth vanadate photoanodes for use in solar water oxidation, *Chem. Soc. Rev.*, 2013, **42**, 2321–2337.
13 L. Zou, H. Wang and X. Wang, High Efficient Photodegradation and Photocatalytic Hydrogen Production of CdS/$BiVO_4$ Heterostructure through Z-Scheme Process, *ACS Sustainable Chem. Eng.*, 2017, **5**, 303–309.
14 M. G. Lee, C. W. Moon, H. Park, W. Sohn, S. B. Kang, S. Lee, K. J. Choi and H. W. Jang, Dominance of Plasmonic Resonant Energy Transfer over Direct Electron Transfer in Substantially Enhanced Water Oxidation Activity of $BiVO_4$ by Shape-Controlled Au Nanoparticles, *Small*, 2017, **13**, 1701644.
15 J. K. Cooper, S. Gul, F. M. Toma, L. Chen, P.-A. Glans, J. Guo, J. W. Ager, J. Yano and I. D. Sharp, Electronic Structure of Monoclinic BiVO4, *Chem. Mater.*, 2014, **26**, 5365–5373.
16 Q. Wang, Y. Li, T. Hisatomi, M. Nakabayashi, N. Shibata, J. Kubota and K. Domen, Z-scheme water splitting using particulate semiconductors immobilized onto metal layers for efficient electron relay, *J. Catal.*, 2015, **328**, 308–315.
17 J. K. Kim, X. Shi, M. J. Jeong, J. Park, H. S. Han, S. H. Kim, Y. Guo, T. F. Heinz, S. Fan, C.-L. Lee, J. H. Park and X. Zheng, Enhancing Mo:$BiVO_4$ Solar Water Splitting with Patterned Au Nanospheres by Plasmon-Induced Energy Transfer, *Adv. Energy Mater.*, 2018, **8**, 1701765.